Simulation of Harmonic Drive in Precision Robotic System

Gang-jun Li
Electromechanical engineering Department,
Chengdu ElectroMechanical College
Chengdu, China

***Abstract*—A simulation model of precise harmonic drives transmission system including the effects of friction and transmission flexibility is developed in this paper. The friction in both motor and load side are analysed, nonlinear friction which include static、Coulomb and viscous friction are described as a function of position and velocity, the periodical part of friction is simulated by Fourier series. The simulation results are identifed by experiments. It shows the effectiveness of the proposed scheme.**

Keywords-simulation; modelling; harmonic drive; friction; precision system l

I. INTRODUCTION

Harmonic drive has captured more and more researcher's attention in the last decades. Because it has many advantages including near-zero backlash, high gear reduction ratio and compact design, it is more and more widely used in precision control systems. For example, in the optoelectronic automation industry, the process of attaching optical fibres to optoelectronic devices requires submicron alignment accuracy in positioning. On the other hand, the nonlinear attributes are responsible for performance degradation. Therefore, a accurate modelling of the system is critical for the use of harmonic drives, this model should include the main nonlinear attributes of the system.

II. FRICTION MODELLING

Friction force is proportional to load, opposes the motion, and is independent of the contact area----this was known to all. Now the static + Coulomb + viscous friction model is most commonly used in engineering.

So far, about thirty friction models have been presented. Dahl concluded that for small motions, a junction in static friction behaves like a spring; he then considered the implications for control. A dynamic friction model was proposed by C. Canudas de Wit et al. [1]. The model, called the LuGre model, captures most of the friction behaviour that has been observed experimentally. This includes the Stribeck effect, hysteresis, spring-like characteristics for stiction, and varying breakaway force, his experimental results validated the LuGre friction model in an adaptive control scheme with friction compensation. Gandhi[2] uses the LuGre model to identify the friction in harmonic drives. The shortcomings of the LuGre model lie in its inability to account for nonlocal memory and in that it cannot accommodate arbitrary displacement force transition curves[3].

In recent years, many other friction models have been proposed[4]. Tariku et al.[5] proposed two dynamic models for simulation of one-dimensional and two-dimensional stick-slip motion. Wu et al.[6] presented a modified Coulomb friction model integrating presliding displacement in the microsliding regime. Popovic et al.[7] noticed that the most of friction models describe friction as a function of velocity only. With harmonic drives, Popovic proposed a new spectral-based modelling technique that ably describes nonlinear friction as a function of position and velocity.

Taghirad[8] developed an overall friction model for harmonic drives and also modelled the harmonic drive including friction and compliance. Tuttle et al.[9] developed a nonlinear harmonic drive model. The latter model captures most nonlinear behaviours, such as kinematic error, friction, and flexibility. However, the above two models do not consider the position dependent friction. Gandhi[10] proposed an overall model for harmonic drives. He modelled all main nonlinear attributes in the harmonic drive, such as kinematic error, hysteresis and friction. He observed the position dependent friction in hannonic drives, and used the Fourier series to model the position dependent friction. He also came up with a new hysteresis model for harmonic drives. In his friction model, he considered one revolution friction on motor side only, and did not observe that the friction in harmonic drives is dependent on load side position also.

III. NONLINEAR ATTRIBUTES OF HARMONIC DRIVES

Harmonic drives are special flexible gear transmission systems that have a non conventional construction with teeth meshing at two diametrically opposite ends. Because of their unique construction and operation, they have many useful properties. However, these drives possess nonlinear transmission attributes that are responsible for transmission performance degradation. The main nonlinear attributes are:

Kinematic error - what harmonic drive literature refers to as kinematic error is a difference between the ideal and the actual output position. However, in harmonic drives, a small amplitude of periodic kinematic error exists between the ideal and the actual output position, and makes the gear ratio dependent on the input position. The error also has a dynamic component.

This work was supported by the Foundation of Sichuan Education Department under Grant No.09ZC24

Flexibility and presliding - flexibility in a harmonic drive results from various compliant elements including the flexspline cup, elliptical ball bearing and gear teeth. Nonlinear interactions of the elliptical ball bearing, the flexspline and the circular spline with friction at the contact surfaces, along with flexibility effects, produce a presliding signature. Presliding is the flexible displacement in harmonic drives. In mechanical systems, presliding makes hysteresis attributes in a system's output.

Friction - friction is a critical problem for precision positioning. Friction in the harmonic drive, as in any other system, produces nonlinear dynamic effects, especially at slow velocities and when there is a reversal in the direction motion. The additional peculiarity of harmonic drive friction is its periodic dependence on the motor or wave generator position, and also on the load or circular spline position. The friction in a harmonic drive is very complicated and has significant influence on positioning.

IV. HAMONIC DRIVE MODELLING EXPLORES

In order to study the model of hamonic drive, we build a set of experimental apparatus. A robotic manipulator with three degrees of freedom was previously developed, it has two arms driven by harmonic drive motors and one linear stage actuated by a timing belt driven lead screw. The robotic manipulator are controled by a computer with an amplifier and an interface card. The interface card includes A/D, D/A and an encoder accessing device. Two capacitance sensors are mounted parallel to the arms of the manipulator and are used to measure the position of the arms. The overall control scheme is illustrated in Fig.1:

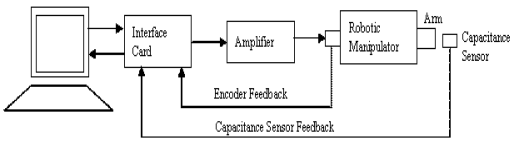

Fig. 1 Overall control scheme

A. Initial modelling approximations

The arms of the manipulator are driven by harmonic drive motors. Because the hysteresis effect in harmonic drives is relatively small, especially in precision impulse control, it can be negligible. A harmonic drive can be modelled as two masses connected with a spring, as shown in Fig.2 . The control input acts on the motor and wave-generator inertia J_m, which is connected via a gear reduction r to the flexspline and arm inertia J_l. The flexibility of the harmonic drive motor plays a significant role in system dynamics and is modelled using a torsional spring that produces a torque T_s •

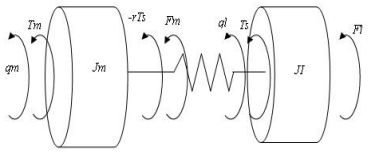

Fig. 2 Harmonic drive model

F_m and F_l stand for frictions in motor side and load side respectively in Fig.2. Newton's second law is used for both motor and load side:

$$J_m\ddot{q}_m = T_m - F_m - T_s \quad (1)$$

$$J_l\ddot{q}_l = T_s - F_l \quad (2)$$

$q_m$and q_l are the positions of motor and load; T_m is the motor input torque; T_s is given by:

$$T_s = K_s(rq_m - q_l) \quad (3)$$

K_s is a spring constant of the harmonic drive.

For the armature controlled motor, motor torque can be written as:

$$T_m = K_m i_a \quad (4)$$

K_m is the motor torque constant, i_a is the armature current. It is apparent that the input voltage is

$$u(t) = i_a R + L\frac{di_a}{dt} + K_b\omega_m \quad (5)$$

where R is armature resistance, L is armature inductance, K_b is voltage constant and ω_m is motor velocity. From the manual, L=2.7mH; it is very small and can be neglected. Then:

$$i_a = \frac{-K_b\dot{q}_m + u(t)}{R} \quad (6)$$

The substitution of (6) into (4) yields

$$T_m = -\frac{K_m K_b}{R}\dot{q}_m + \frac{K_m}{R}u(t) \quad (7)$$

The substitution of (7) and (3) into (1) and (2) yields

$$J_m\ddot{q}_m = -F_m - rK_s(r\ddot{q}_m - q_l) - \frac{K_m K_b}{R}\dot{q}_m + \frac{K_m}{R}u(t) \quad (8)$$

$$J_l\ddot{q}_l = -F_l + K_s(rq_m - q_l) \quad (9)$$

B. Friction modelling

The measurement verifies the friction in the harmonic drive is quite position dependent, the friction varies periodically and the period is 2π , so the friction can be modelled as follows: the average of the friction can be modelled as a parabolic curve, periodical changes of friction can be modelled as a Fourier series, and the viscous effect can be modelled as a viscous coefficient multiplied by motor velocity.

The average Coulomb friction is simulated using a second order polynomial:

$$f_{aver} = s_1 q_m^2 + s_2 q_m + s_3 \quad (10)$$

By using the 'fminunc' function in Matlab, it is possible to minimize the Euclidian norm of error between the simulation and experimental data. The coefficients obtained are:

S_1= 1.5738e-006 S_2 = -3.7901e-004 S_3 = 0.0720

The simulation and experimental data are plotted in Fig.3.

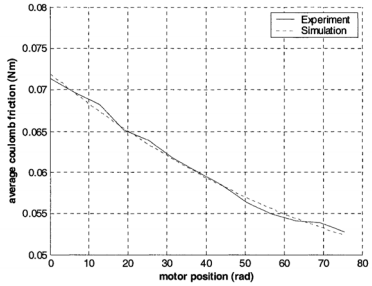

Fig. 3 Average Coulomb friction

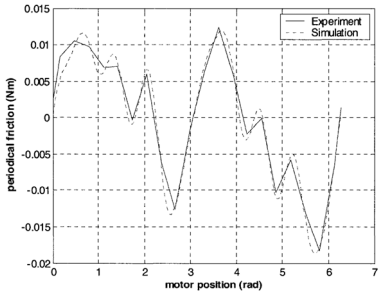

Fig. 4 Periodical friction

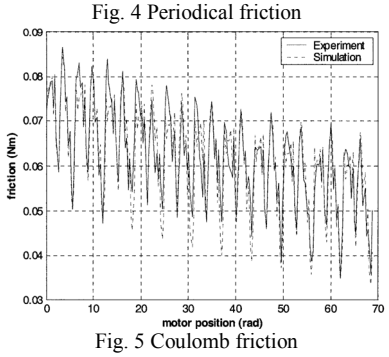

Fig. 5 Coulomb friction

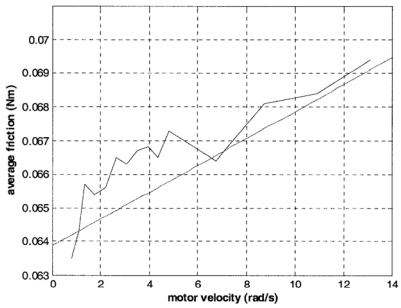

Fig. 6 Viscous friction

For the periodical term of friction, the first 2π is chosen for our simulation period. In the period of 0-2π, we remove the average of the friction from the experimental data. Using the 10th order of Fourier series to simulate it, the friction can be expressed as:

$$f_{peri} = \frac{a_0}{2} + \sum_{k=1}^{10}[a_k \cos(kq_m) + b_k \sin(kq_m)] \quad (11)$$

The Fourier coefficients (a_k, b_k) are obtained using numerical integration:

$$a_k = \frac{1}{\pi}\int_0^{2\pi} f_{peri}(q_m)\cos(kq_m)dq_m \quad (12)$$

$$b_k = \frac{1}{\pi}\int_0^{2\pi} f_{peri}(q_m)\sin(kq_m)dq_m \quad (13)$$

The experiment and simulation for periodical friction in the first 2π are shown in Fig.4.

The Coulomb friction is the sum of the periodical term and average term:

$$f_{coul} = f_{aver} + f_{peri} = s_1 q_m^2 + s_2 q_m + s_3 + \frac{a_0}{2} + \sum_{k=1}^{10}[a_k \cos(kq_m) + b_k \sin(kq_m)] \quad (14)$$

The final simulation result of Coulomb friction is shown in Fig.5. The experimental data is also plotted for comparison.

By measuring the friction in the work-range at different velocities and calculating the average value of friction, a viscous tendency can be found and it is illustrated in Fig.6. The minimization of the Euclidian norm of error between the simulation and experimental data points is also shown in the same Figure:

$$f_{visc} = b_m \dot{q}_m + B \quad (15)$$

b_m = 0.0004 Nm/rad/s, B = 0.0642

The viscous coefficient b_m is 0.0004 Nm/rad/s.

Static friction can only be measured while the motor is moving. Therefore, only a manual measurement method can be used. Because noise exists in the system, and the kinematic error changes irregularly for different positions, static friction cannot be averaged between sampling times. In this paper, only the static friction in the first π radian range is measured. The result illustrates that there is a consistency between static and Coulomb friction. The average static friction is larger than that of Coulomb by about 3.88%. We can simply assume that the static friction is 1.0388 times that of the Coulomb friction at any position. Static friction $f_{sm}(q_m)$ can therefore be expressed as

$$f_{sm}(q_m) = (s_1 q_m^2 + s_2 q_m + s_3 + \frac{a_0}{2} + \sum_{k=1}^{10}[a_k \cos(kq_m) + b_k \sin(kq_m)]) \times 1.0388 \quad (16)$$

C. *Average friction model*

The measured friction is quite position dependent. In the precision position control, the control range is small, static friction and Coulomb friction can be averaged and considered constants. The friction used in equation (8) and (9) can be modelled as static + viscous + coulomb. Thís model is accurate enough for most engineering applications. The motor side and load side frictíon can be written as:

$$\begin{aligned} F_m &= -\psi_m && \text{if } \dot{q}_m = 0,\ |\psi_m| \le f_{sm} \\ F_m &= -\mathrm{sgn}(\psi_m) f_{sm} && \text{if } \dot{q}_m = 0,\ |\psi_m| > f_{sm} \\ F_m &= -\mathrm{sgn}(\dot{q}_m) f_{cm} - b_m \dot{q}_m && \text{if } |\dot{q}_m| > 0 \\ \psi_m &= -rK_s(rq_m - q_l) + \frac{K_m}{R}u(t) \end{aligned} \quad (17)$$

And

$$F_l = -\psi_l \quad \text{if } \dot{q}_l = 0,\ |\psi_l| \le f_{sl}$$

$$F_l = -\mathrm{sgn}(\psi_l) f_{sl} \qquad \text{if } \dot{q}_l = 0,\ |\psi_l| > f_{sl}$$
$$F_l = -\mathrm{sgn}(\dot{q}_l) f_{cl} - b_l \dot{q}_l \quad \text{if } |\dot{q}_l| > 0$$
$$\psi_l = K_s (r q_m - q_l) \tag{18}$$

ψ_m is input torque when $\dot{q}_m = 0$, ψ_l is the spring torque when $\dot{q}_l = 0, f_{sm}$ and f_{cm} are motor side static friction and Coulomb friction. f_{sl} And f_{cl} are load side static friction and Coulomb friction.

D. State equations

We define the state variables as:

$$\begin{bmatrix} x_1 \\ x_2 \\ x_3 \\ x_4 \end{bmatrix} = \begin{bmatrix} q_m \\ \dot{q}_m \\ q_l \\ \dot{q}_l \end{bmatrix} \tag{19}$$

Then, the equations of (8) and (9) can be written in state variable format：

$$\begin{bmatrix} \dot{x}_1 \\ \dot{x}_2 \\ \dot{x}_3 \\ \dot{x}_4 \end{bmatrix} = \begin{bmatrix} x_2 \\ -\frac{F_m}{J_m} - \frac{rK_s}{J_m}(rx_1 - x_3) - \frac{K_m K_b}{J_m R} x_2 + \frac{K_m}{J_m R} u(t) \\ x_4 \\ -\frac{F_l}{J_l} + \frac{K_s}{J_l}(rx_1 - x_3) \end{bmatrix} \tag{20}$$

E. Simulation and Experiment

In order to overcome the static friction, a square pulse amplitude is fixed in four times of static friction h=4Vs,Vs is the voltage required to overcome static friction. When the pulse width is W=lms, the open loop simulation and experimental response to the square pulse are shown in Fig.7 and Fig.8. It is apparent that the simulation is consistent with the experiment.

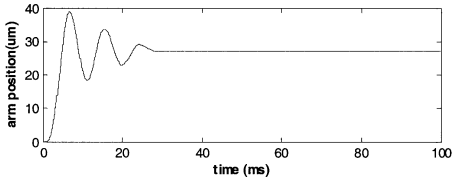

Fig.7 Square pulse simulation response

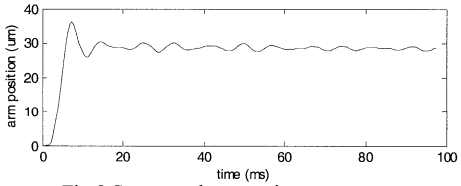

Fig.8 Square pulse experiment response

V. CONCLUSION

In this paper, a simulation model of harmonic drives in precision robotic system has been developed. The main nonlinear attributes of harmonic drives are analysed, a function of position and velocity is used to describe nonlinear friction, experiments and simulation results validate the model, it will benefit the development of control method and application for harmonic drives in precision system.

REFERENCES

[1] Carlos Canudas de wit, Olsson,H., Astrom, K.J., Lischinsky, P., "A New Model for Control of Systems with Friction", IEEE Transaction Automatic Control Vol. 40, No. 3, Mar. 1995 PP 419-425

[2] Gandhi, P.S., Ghorbel, F.H., Dabney, J. , "Modelling, Identification, and Compensation of Friction in Harmonic Drives", Proc. Of 41st IEEE Conf. On Decision and Control. Dec. 2002, Las Vegas, PP160-166

[3] Marton, L. and Lantos, B. "Modeling, identification, and compensation of stick–slip friction", IEEE Trans. Ind. Electronics, 2007, 54(1), pp511–521

[4] Lemmer L.and Kiss B., "Modeling, Identification, and Control of Harmonic Drives for Mobile Vehicles", in Proceedings of the IEEE 3rd International Conference on Mechatronics, Budapest, July 2006, pp. 369–374.

[5] Tariku, F.A., Rogers, R.J.,"Improved Dynamic Friction Models for Simulation of One-Dimensional and Two-Dimensional Stick-Slip Motion", Joumal of Tribology Oct. 2001 , Vol. 123 pp 661-669

[6] Wu, R.H., Tung, P.c., "Studies of Stick-Slip Friction, Presliding Displacement, and Hunting." J. of Dynamic Systems, Measurement, and Control, Mar. 2002, Vo1. 124, PP 111-117

[7] Popovic, M.R., and Goldenberg, A.A., " Modelling of Friction Using Spectral Analysis", IEEE Transaction on Robotics and Automation, Vol.14, No.l , Feb.1998, PP 114-122

[8] Taghirad, H.D., Belanger, P.R., "Model1ing and Parameter Identification of Harmonic Drive Systems" J. of Dynamic Systems, Measurement, and Control, Dec.1998, Vol. 120,PP439-444

[9] Tuttle, T.D., Seering, W.P., " A Nonlinear Model of a Harmonic Drive Gear Transmission", IEEE Transaction on Robotics and Automation Vol. l2, No. 3 June 1996, PP 368-374

[10] Gandhi P.S., and Ghorbel F., "High-speed precision tracking with harmonic drive systems using integral manifold control design ", International Journal of Control, Volume 78, Issue 2 January 2005 , pp 112 - 12